

**THE EFFECTS OF PHOTOBIOREACTOR  
AVERAGE SHEAR RATE ON CHITIN  
NANOFIBER PRODUCTION CHARACTERISTICS  
OF THE DIATOM *CYCLOTELLA CRYPTICA***

A Thesis Submitted to  
the Graduate School of Engineering and Sciences of  
İzmir Institute of Technology  
in Partial Fulfillment of the Requirements for the Degree of  
**MASTER OF SCIENCE**  
in Biotechnology

by  
Cemre AĞAOĞLU

October 2024  
İZMİR

We approve the thesis of **Cemre AĞAOĞLU**

**Examining Committee Members:**

---

**Assoc. Prof. Dr. Altan ÖZKAN**

Environmental Engineering, İzmir Institute of Technology

---

**Assist. Prof. Dr. Benay UZER YILMAZ**

Mechanical Engineering, İzmir Institute of Technology

---

**Assoc. Prof. Dr. Sibel UZUNER**

Food Engineering, İzmir Institute of Technology

---

**Prof. Dr. Murat ELİBOL**

Bioengineering, Ege University

---

**Prof. Dr. Sait SARGIN**

Bioengineering, Bursa Technical University

11 October 2024

---

**Assoc. Prof. Dr. Altan ÖZKAN**

Supervisor, Environmental Engineering  
İzmir Institute of Technology

---

**Assist. Prof. Dr. Benay UZER YILMAZ**

Co-Supervisor, Mechanical Engineering  
İzmir Institute of Technology

---

**Assist. Prof. Dr. Arzu UYAR**

Head of the Department of Biotechnology

---

**Prof. Dr. Mehtap EANES**

Dean of the Graduate School

## ACKNOWLEDGMENTS

I would like to express my deepest gratitude to my supervisors Assoc. Prof. Dr. Altan Özkan and Assist. Prof. Dr. Benay Uzer Yılmaz for their alembicated guidance, immense amount of patience and empathic accuracy.

I would like to express my sincere appreciation to the Abdi İbrahim Foundation for allocating funds to support young people pursuing careers in the field of biotechnology.

I would like to thank The Scientific and Technological Research Council of Türkiye for funding the 219M564 project which enabled me to conduct my experiments.

I would like to thank Afife Güleç, Evrim Balcı, Dane Rusçuklu, Yekta Günay, Özgür Yılmazer, Murat Delman and Zehra Sinem Yılmaz for their assistance in making the best use of IZTECH Integrated Research Center's technical infrastructure.

I would like to thank my labmate Tuğçe Sezgin for taking all necessary precautions to extend the lifespan of communal equipment in the Microalgal Biotechnology Laboratory.

I would like to thank Mustafa Kocababaş and Peter Tarkov for generously sharing very important technical information regarding microscopic imaging.

I would like to thank Dr. Leyla Gamze Tolun, Prof. Dr. Andrew Allen and Prof. Dr. Zlatko Levkov for the support they gave me to attend scientific meetings which broadened my research horizons.

I would like to thank Gürdal Ersoy, Peyman Yüksel, Yiğit Karacan and Ercan Çavuş for their support in accelerating the repair and return delivery process of laboratory glassware crucial for the continuation of my experiments.

I would like to thank Kaniye Güneş for shedding light on my way and holding space for me to calmly reconsider the lightning-fast decisions I made while I was dealing with concurrent crises.

I would like to thank my soul sister Merve Aksoy for keeping the ears of her heart wide open and taking time to listen to me non-judgmentally whenever I needed. Even though we are miles apart in different countries, she made me feel like she was right beside me in every mental breakdown I went through during the time I spent at IZTECH.

I dedicate this work to my mom who noticed my innate curiosity towards microcosmos and gifted me a mini microscope when I was just 9 years old. Thank you, mom, for being my vital force and greatest inspiration for all the good things I have achieved so far.



## ABSTRACT

### THE EFFECTS OF PHOTOBIOREACTOR AVERAGE SHEAR RATE ON CHITIN NANOFIBER PRODUCTION CHARACTERISTICS OF THE DIATOM *CYCLOTELLA CRYPTICA*

Chitin is a natural biopolymer with significant potential for use in biomedical applications. Currently, majority of the commercially available chitin is based on crustacean shell waste generated by seafood industry. Diatoms belonging to *Cyclotella* and *Thalassiosira* genera have the unique ability to extrude the chitin nanofibers out of their cell walls through the tubular openings, called fultoportulae and thus eliminate the need for application of harsh extraction methods for chitin harvesting.

In this study, the effects of variation in aeration-induced shear rate have on the chitin nanofiber productivity of diatom *Cyclotella cryptica* CCMP 333 were investigated by following a two-stage silicon addition protocol (0.20 mM in first stage and 1.80 mM in second stage) in a bubble column photobioreactor. During the first stage, the aeration flow rate was 0.5 vvm and during the second stage, *Cyclotella cryptica* cells were exposed to different gas aeration flow rates, 0.25 vvm, 1 vvm and 1.5 vvm.

The highest chitin concentration of 852 mg/L was obtained following the combined effects of silicon deplete growth conditions and a second stage aeration rate of 1 vvm. The concentrations of free chitin and cell bound chitin in suspensions were determined on samples collected during the stationary phase from all cell suspensions started with the same initial cell densities. The results showed an inversely proportional relation between the ratio of cell-bound chitin nanofibers and increased aeration flow rate. Further studies addressing yield enhancement are required for ensuring the viability of commercial scale diatom-based chitin production facilities.

## ÖZET

### KABARCIK KOLON FOTOBIYOREAKTÖR ORTALAMA KESME HİZİNİN *CYCLOTELLA CRYPTICA* DİATOMUNUN KİTİN NANOFİBERİ ÜRETİM ÖZELLİKLERİNE ETKİLERİ

Kitin biyomedikal uygulamalar açısından çok yüksek potansiyelli doğal bir biyopolimerdir. Halihazırda, ticari kitin üretiminin çoğunluğu deniz ürünlerini endüstrisi tarafından işlenen kabuklu deniz canlılarının atıkları kullanılarak yapılmaktadır. Diatom cinslerinden *Cyclotella* ve *Thalassiosira* kitin nanofiberlerini direkt olarak hücre duvarları üzerinde bulunan fultoportula adı verilen açıklıklardan dış ortama sentezleyebildikleri için kitin hasatı için sert ektraksiyon koşulları uygulanması gerekliliğini ortadan kaldırmaktadır. Bu çalışmada, *Cyclotella cryptica* CCMP 333 hücrelerinin kitin üretkenliğinin kabarcık kolon fotobiyoreaktörün havalandırma hızındaki farklılıktan kaynaklı maruz kaldıkları hidrolik kesme kuvvetinden nasıl etkilendiği iki aşamalı bir kültürasyon protokolü (birinci aşamada 0,020 mM silikon takviyesini müteakiben ikinci aşamada 1,80 mM silikon takviyesi) uygulanarak araştırılmıştır. Hücrelerin silikon starvasyonuna maruz bırakıldığı birinci aşamada havalandırma hızı 0,5 vvm olarak sabit tutulmuştur, 1,80 mM silikon takviyesinin ardından havalandırma hızlarının 0,25 vvm, 1 vvm ve 1,5 vvm olarak değiştirildiği 3 ayrı fotobiyoreaktör düzeneği kurulmuştur.

Bu çalışma kapsamında ulaşılan maksimum kitin üretkenliği 852 mg/L olmuştur ve bu konsantrasyona silikon starvasyon aşamasında 0,5 vvm ile havalandırılan ve ardından 1,8 mM silikon takviyesi ile eş zamanlı olarak havalandırma hızının 1 vvm olarak değiştirildiği deney grubunda saptanmıştır. *Cyclotella cryptica* CCMP 333 hücre süspansiyonlarında serbest olarak ve hücreye bağlı olarak buluna kitin konsantrasyonları durağan faz sürecinde toplanan numuneler kullanılarak belirlenmiştir. Hücreye bağlı kitin nanofiberlerin konsantrasyonu ile havalandırma akış hızları arasında ters orantı olduğuna dair elde edilen sonuçlar büyük ölçekli diatom üretim tesislerinde hasatlanacak kitin nanofiberi miktarının maksimizasyonu için geliştirilecek stratejilere katkı sağlayacaktır.

## TABLE OF CONTENTS

LIST OF FIGURES.....	viii
LIST OF TABLES.....	x
CHAPTER 1 INTRODUCTION .....	12
CHAPTER 2 METHODOLOGY.....	12
2.1. Preparation of Culture Media.....	12
2.2. Photobioreactor Setup and Process Parameters.....	12
2.3. Dissolved Nutrient Concentration Measurements.....	14
2.4. Cell Number Density Measurements.....	15
2.5. Chitin Nanofiber Concentration Measurements.....	15
CHAPTER 3 RESULTS AND DISCUSSION .....	19
3.1. Effects of Different Gas Flow Rates on Cell Densiy.....	19
3.2. Effects of Different Gas Flow Rates on Chitin Productivity .....	20
3.3. Chitin Nanofiber Length and Diameter Distribubtions .....	22
3.4. Effects of Different Gas Flow Rates on Fultoportulae Number.....	25
3.5. Effects of Different Gas Flow Rates on the Concentrations of Cell Bound Chitin Nanofibers and Free Chitin Nanofibers .....	26
CHAPTER 4 CONCLUSION .....	27
REFERENCES.....	29
APPENDICES	
APPENDIX A.....	36

## LIST OF FIGURES

<u>Figure</u>	<u>Page</u>
Figure 1.1. Scanning electron microscopy image of <i>Cyclotella cryptica</i> .....	2
Figure 1.2. Chitin synthesis in diatoms.....	2
Figure 1.3. Fibrin polymerization upon chitin exposure.....	3
Figure 1.4. $\alpha$ , $\beta$ and $\gamma$ allomorphs of chitin.....	4
Figure 1.5. Chitins extracted from different organisms .....	5
Figure 1.6. Chitin in crustacean exoskeleton .....	8
Figure 1.7. Chitin in fungal cell wall.....	8
Figure 1.8. Chitin in insect peritrophic matrix.....	9
Figure 2.1. Photobioreactor setup used for <i>Cyclotella cryptica</i> cultivation.....	14
Figure 2.2. Appearance of Evans Blue on Thoma chamber and stained cell.....	15
Figure 2.3. Chitin nanofiber images obtained by scanning electron microscopy.....	16
Figure 2.4. Dislodged chitin nanofibers.....	17
Figure 2.5. Cell-bound chitin nanofibers.....	18
Figure 3.1. Cell number density vs. time for different aeration gas flow rates.....	19
Figure 3.2. Chitin production per cell vs. time for different aeration gas flow rates.....	20
Figure 3.3. Chitin concentration with respect to cultivation time .....	21
Figure 3.4. Boxplot distribution of the diameters of chitin nanofibers secreted by <i>Cyclotella cryptica</i> cells during cultivation at different aeration gas flow rates.....	23
Figure 3.5. Boxplot distribution of the lengths of chitin nanofibers secreted by <i>Cyclotella cryptica</i> cells during cultivation at 0.25 vvm.....	23

<b><u>Figure</u></b>	<b><u>Page</u></b>
Figure 3.6. Boxplot distribution of the lengths of chitin nanofibers secreted by <i>Cyclotella cryptica</i> cells during cultivation at 1 vvm.....	24
Figure 3.7. Boxplot distribution of the lengths of chitin nanofibers secreted by <i>Cyclotella cryptica</i> cells during cultivation at 1.5 vvm.....	24
Figure 3.8. Concentration of cell-bound and free chitin nanofibers at different aeration gas flow rates.....	26



## LIST OF TABLES

<u>Table</u>	<u>Page</u>
Table 1.1. Chitin Content in Different Organisms.....	7
Table 1.2. Environmental Impacts of Chitin Production by Fungi and Shrimp.....	10
Table 3.1. Average Length of Chitin Nanofibers for Each Experimental Group.....	13
Table A.1. Salts Added to the Culture Media.....	36
Table A.2. Trace Metals Added to the Culture Media.....	36
Table A.3. Vitamins Added to the Culture Media.....	36
Table A.4. Major Nutrients Added to the Culture Media.....	37

# CHAPTER 1

## INTRODUCTION

Diatoms are silicified microorganisms found in many different marine, freshwater and terrestrial habitats. Due to the presence of highly efficient carbon dioxide concentration mechanisms, diatoms contribute to the primary production at varying rates depending on the habitats in which they live, e.g. more than 85% for the North Pacific Ocean and Southern Ocean, and up to 40% for the Equatorial and North Central Atlantic (Rousseaux, C.S. & Gregg, W., 2013).

In addition to their crucial role in ecosystems, diatoms are propitious for biotechnological applications because almost all components of diatom biomass contribute to the development of integrated biorefinery approaches to produce high quality bioproducts (Wang, J. and Seibert, M. 2017). The presence of advanced mechanical defense mechanisms, unique structural features and modifiable pore structures make diatoms preferable microorganisms to be used as cell machinery for producing biomaterials such as chitin (Sharma et al. 2021).

Diatom strains belonging to *Cyclotella* and *Thalassiosira* genera have the capability to synthesize chitin, poly-(1→4)- $\beta$ -N-acetyl-D-glucosamine, which is a biopolymer with a wide range of applications e.g. drug delivery, production of bio-stimulants, smart packaging films, surgical sutures, wound dressings and tissue engineering scaffolds. The chitin market is continuously expanding and expected to reach 2941 million USD by 2027 (Mahmood et al. 2022). The purity scale of the chitin directly controls its potential to be used in applications requiring high quality products and the income generated from the product (Aranaz, I. et al. 2009). Currently, the sales price of 1 kg of Crustacean based chitin powder varies between 135-841 USD depending on the purity (ChitoLytic & VWR International, 2024).

As pointed with the blue arrows in the scanning electron microscopy image presented as Fig 1.1., *Cyclotella cryptica* cells extrude chitin from the tubular openings called fultoportulae found on the outer region of the valve (Özkan, A. 2023).

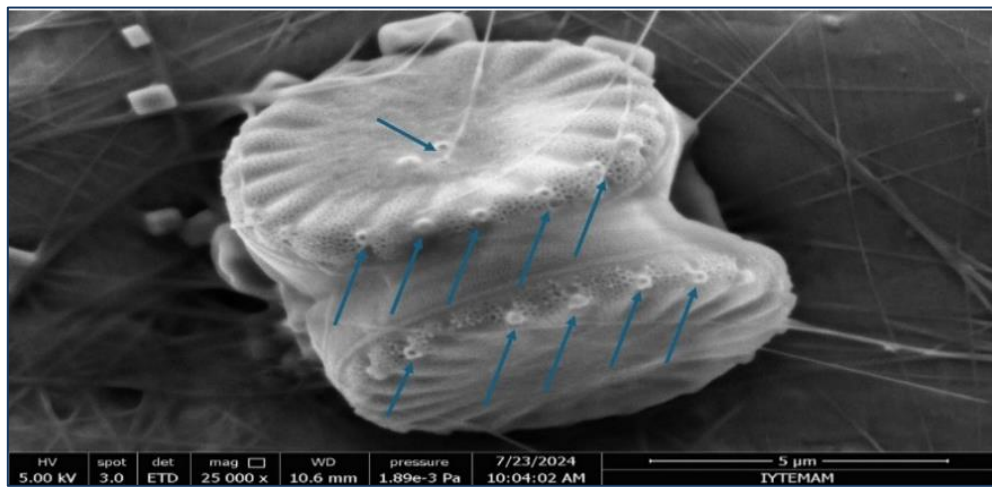


Figure 1.1. Scanning electron microscopy image of *Cyclotella cryptica*.

The schematic illustration showing the transformation of carbon dioxide and nitrate into biomass production and chitin synthesis is given below. The formation of chitin strands takes place in the chitinogenic envelope with the involvement of putative enzymes and monomer units of uridine diphosphate N-acetylglucosamine (Jeffreys, C. et al. 2015). Therefore, following biosynthesis, the chitin fibers are immediately released from the cells.

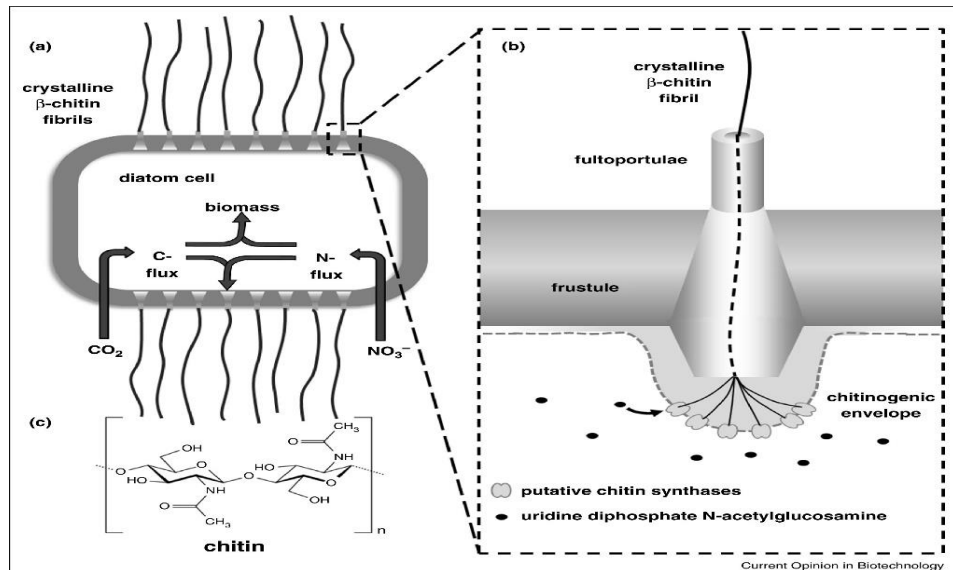


Figure 1.2. Chitin Synthesis in Diatoms (Source:Jeffreys, C. et al. 2015).

Diatom-originated chitin containing products are currently commercially available (e.g. MRDH® (modified rapid deployment hemostat) and SyvekNT® produced by Marine Polymer Technologies Inc.) and mostly used for ensuring hemostasis after variceal bleeding, splenic hemorrhage and cardiac catheterization (Morganti, P. et al. 2006). Fibrin polymerization in human whole blood sample upon chitin contact is shown in Figure 1.3.

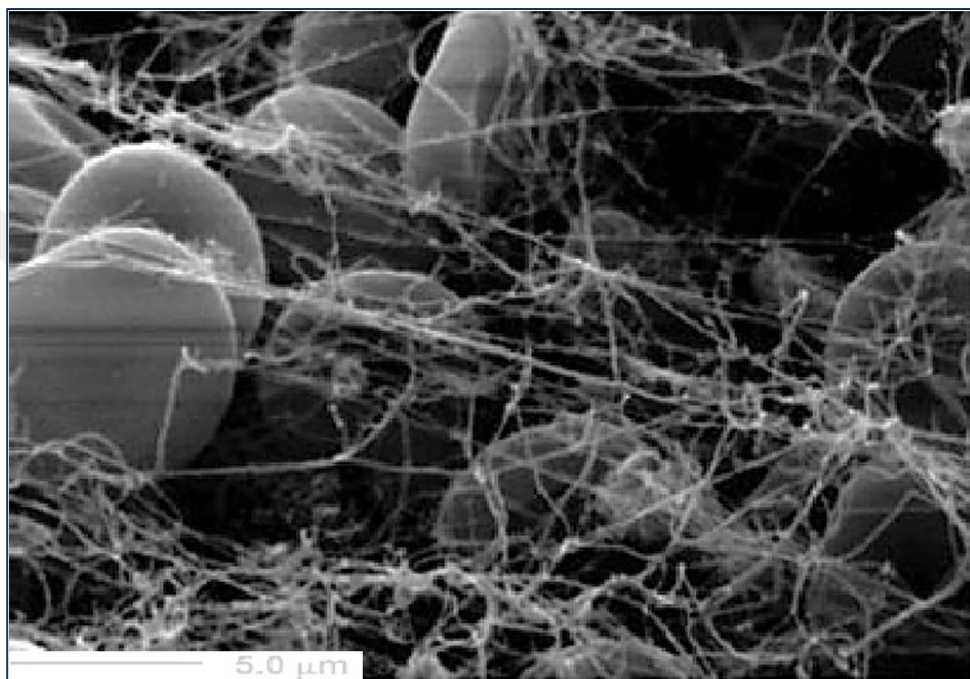


Figure 1.3. Fibrin polymerization upon chitin exposure (Source: Morganti, P. et al. 2006).

Among three polymorphic forms of chitin, alpha ( $\alpha$ ), beta ( $\beta$ ) and gamma ( $\gamma$ ), the  $\gamma$ -chitin is the least common form in nature. As can be seen in Figure 1.4, while  $\gamma$ -chitin has both parallel and antiparallel chains,  $\alpha$ -chitin only has antiparallel chains and  $\beta$ -chitin only has parallel chains. Due to the abundance of inter chain hydrogen bonds,  $\alpha$ -chitin is thermodynamically more stable than  $\beta$ -chitin (Moon, H. et al. 2019), while  $\beta$ -chitin has advantages over  $\alpha$ -chitin in terms of solubility and reactivity (Hou et al. 2021). Since it is not possible to convert  $\alpha$ -chitin to  $\beta$  form, (on the contrary  $\beta$ -chitin can be converted to  $\alpha$ -chitin), production of  $\beta$ -chitin is obviously going to be more and more important in the future (Sulthan R. et al. 2023).

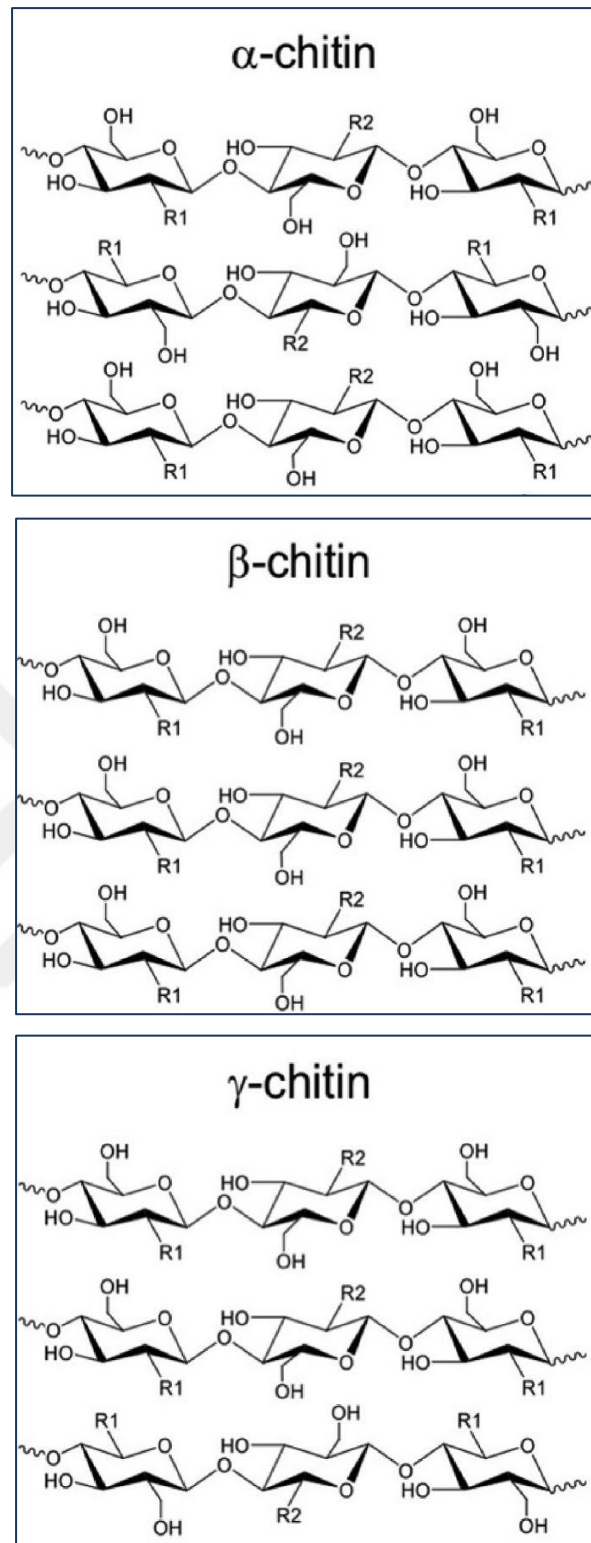


Figure 1.4.  $\alpha$ ,  $\beta$  and  $\gamma$  allomorphs of chitin (Source: Jin, S. & Spontak, R. 2023).

Since their structural, morphological and physiochemical properties differ from each other, chitins originate from different organisms and even different parts of the same organism have distinct features to be tailored for specific applications. For instance, if the final product requires higher thermal resistance, krill chitin, which contains antiparallel chains and extra interchain hydrogen bonds, is better than squid chitin which contains parallel chains (Wysokowski, M. et al. 2015). Hydrogels with tailor-made swelling properties are yet another example. Since  $\alpha$ -chitin has lower susceptibility to swelling than  $\beta$ -chitin (Romay, A. et al. 2023),  $\alpha$ -chitin containing hydrogels are better for internal soft-tissue wounds, while  $\beta$ -chitin containing hydrogels are suitable for full-thickness skin wounds (Feng, W. et al. 2023). Transparency is another important feature for observation of the wound without requiring removal of the wound dressing (Xie, G. et al. 2022). As can be seen in Figure 1.5., upon exposure to same ultrasound treatment,  $\beta$ -chitin extracted from squid pen forms stable and transparent suspension, while  $\beta$ -chitin extracted tubeworm and  $\alpha$ -chitin extracted separately from crab tendon and shell form white suspensions (Liao, J. et al. 2023).

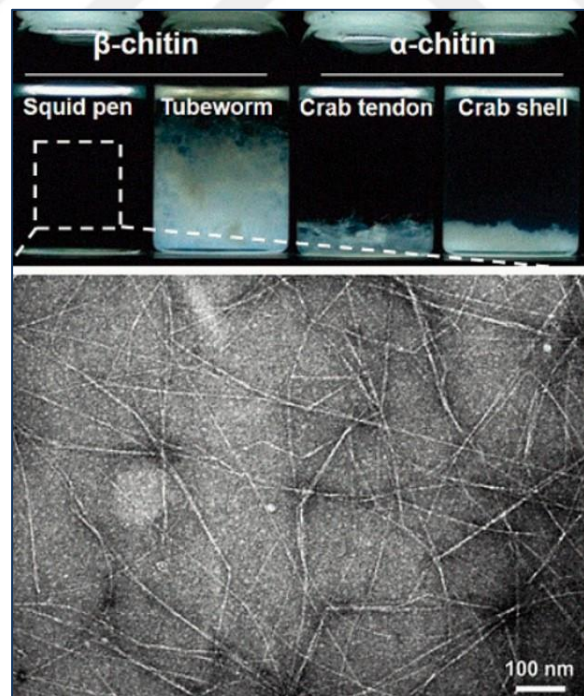


Figure 1.5. Chitins extracted from different organisms (Source:Liao, J. et al. 2023).

Among all the  $\beta$ -chitin bearing organisms, tubeworms are the most difficult to cultivate outside their native habitats, deep-sea ecosystems. Although there are publications reporting laboratory scale cultivations, there is no wide-scale system available for commercial scale production as it is available in diatoms (Miyake, H. et al. 2006).

The foremost advantage of diatoms over other  $\beta$ -Chitin bearing organisms, e.g. tubeworms, bivalve shells, insects, squid and cuttlefish (Rajan, D.K. et al. 2023 and Yu, A. et al. 2024), is the ease of chitin harvest because in other  $\beta$ -Chitin bearing organisms, chitin is embedded in a complex matrix and associated with proteins, minerals and pigments. Regardless of the type of method used, all extraction processes affect the degree of acetylation, molecular weight and mechanical properties of the final product (Abidin, N.A.Z. et al. 2020).

The populations of  $\beta$ -Chitin bearing organisms belonging to Mollusca phylum (e.g. squid from Cephalopoda class, and oyster from Bivalvia class), fluctuate due to extreme rises in ocean temperature (Green, T.J. et al. 2019 and Liu, Y. et al. 2023) and expansion of hypoxic and hypercapnic zones, attributable to human-induced greenhouse gas emissions and alteration in natural biogeochemical cycle of nitrogen and phosphorus within the oceans(Rosa, R. et al 2012 and Beniash, E. et al. 2010).

Moreover, hunting these organisms that are already under the negative influence of habitat destruction and overexploitation, for chitin production, will have negative effects both on the fragile balance of marine ecosystems and seafood prices since cephalopods cover significant amount of dietary protein intake for certain human populations (Mouritsen O.G. and Styrbaek, K. 2018). Even though various aquaculture facilities have recently been established to meet the increasing seafood consumption demand, cephalopod-based chitin production is still less advantageous than diatom-based chitin production, because diatoms grow much more rapidly than cephalopods whose life cycle varies from 4 months to 18 months (Vidal, E.A.G. et al. 2014).

The primary source of commercially available alpha ( $\alpha$ ) chitin is crustacean shell waste generated by the seafood industry (Yadav, M. et al. 2019) and the other promising but not yet commercialized sources are fungal species and insects. The chitin contents of different crustaceans and insects with respect to dry weight of exoskeletons and fungi with respect to dry weight of mycelium compiled in table 1.1. presented on the following page (Hamed, I. et al. 2016 and Mario, F.D. et al. 2008).

Table 1.1. Chitin Content in Different Organisms

	w (chitin) /%
<i>Euphausia superb</i> (krill)	24.00
<i>Nephrops norvegicus</i> (lobster)	69.80
<i>Crangon crangon</i> (shrimp)	17.80
<i>Chionoecetes opilio</i> (crab)	26.60
<i>Blatella sp.</i> (cockroach)	18.40
<i>Pieris sp.</i> (butterfly)	64.00
<i>Bombyx sp.</i> (silkworm)	44.20
<i>Galleria sp.</i> (wax moth)	33.70
<i>Armillaria mellea</i> (honey mushroom)	11.10 ± 1.30
<i>Lentinula edodes</i> (shiitake mushroom)	10.10±1.00
<i>Pleurotus ostreatus</i> (oyster mushroom)	15.30± 2.20
<i>Pleurotus eryngii</i> (king trumpet mushroom)	8.70 ± 1.10

As shown in Figure 1.5., Figure 1.6. and Figure 1.7., as in crustaceans, chitin found in fungi and insects, also must be extracted from a complex matrix and applications of multi-stage extraction procedures inholding harsh conditions cannot be avoided.

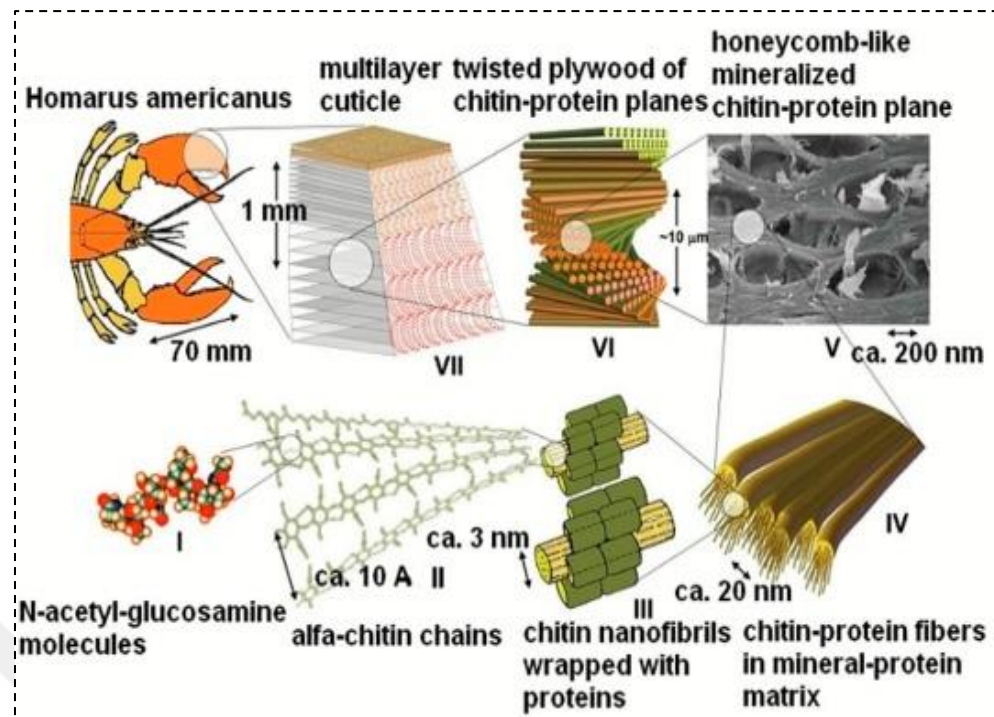


Figure 1.6. Chitin in crustacean exoskeleton (Source: Raabe,D. et al. 2007).

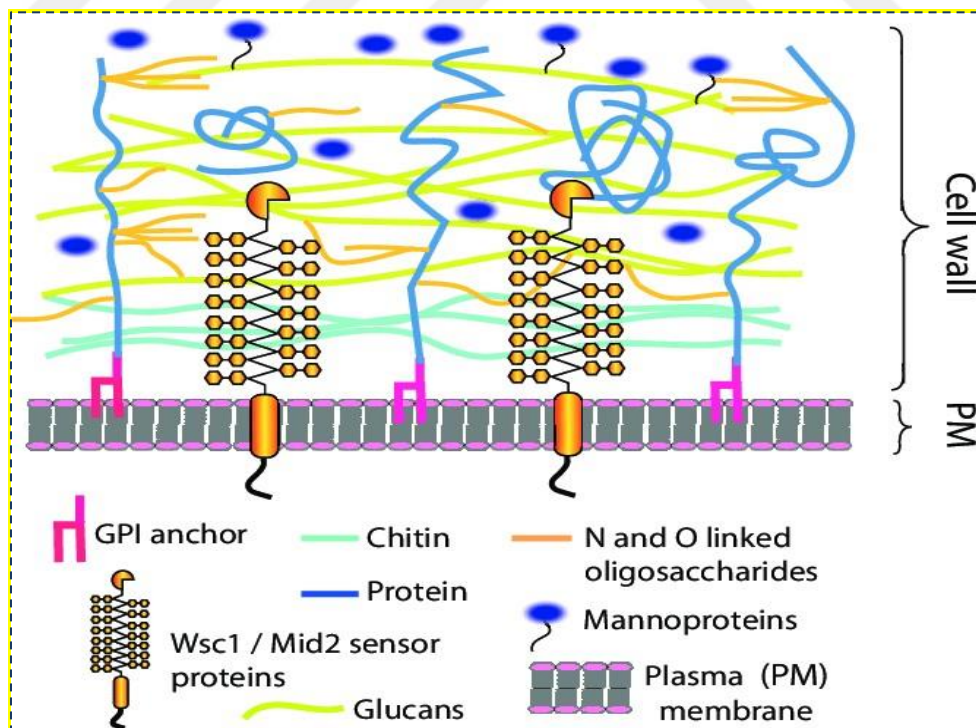


Figure 1.7. Chitin in fungal cell wall (Source: Lubarda, V. et al. 2014).

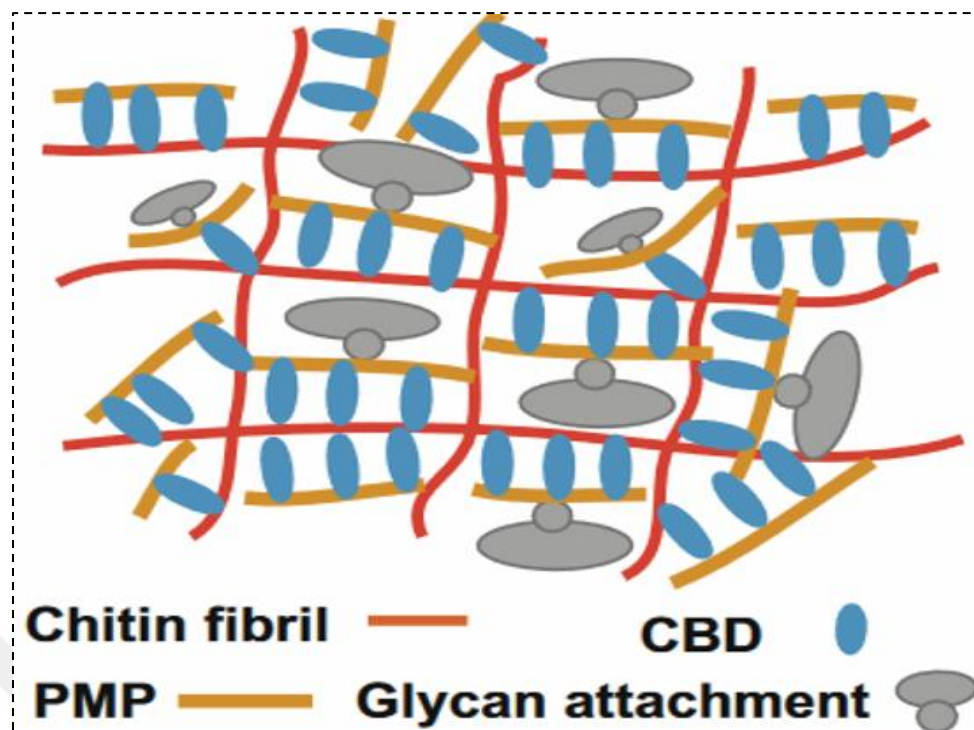


Figure 1.8. Chitin in insect peritrophic natrix (Source: Zhao, X. et al. 2019).

In addition to the harsh extraction conditions reducing the quality of the final product, the environmental effects of current crustacean based chitin production techniques necessitate development of alternative chitin production methods. The environmental advantages of fungal chitin-based nanomaterial production over shrimp chitin-based nanomaterial production are listed in table 1.2 on the following page(Berroci, M. et al. 2022).

Even though the exact reason for chitin nanofiber production by certain diatom strains is not fully disclosed, emerging comprehensive literature on the positive environmental impacts of diatoms and diatom based  $\beta$ -chitin nanofiber production increases the potential of diatom cell factory platforms to be considered as a worthwhile investment. The improvement of survival rate through adaptation to fluctuating conditions in hostile environments by maintaining buoyancy and modulating sinking velocities are among the most accepted explanations for chitin productivity in marine diatoms (Gooday L. et al. 1985)

Table 1.2. Environmental Impacts of Chitin Production by Fungi and Shrimp

Impact	Production of Fungi Originated Chitin Nanofiber	Production of Shrimp Originated Chitin Nanocrystal	Units
Stratospheric ozone depletion	9.97	651.30	$10^{-6}$ kg CFC11 equivalent
Global warming	18.45	906.77	kg CO <sub>2</sub> equivalent
Freshwater ecotoxicity	6.35	402.91	$10^{-1}$ kg 1,4-DCB
Marine ecotoxicity	86.99	5415.17	$10^{-2}$ kg 1,4-DCB
Freshwater eutrophication	18.61	823.50	$10^{-3}$ kg P equivalent
Marine eutrophication	15.13	872.96	$10^{-4}$ kg N equivalent
Fine particulate matter formation	27.93	1522.58	$10^{-3}$ kg PM 2.5 equivalent
Water consumption	1.01	21.44	m <sup>3</sup>

Depending on temperature, pressure and salinity, the density of sea water fluctuates between 1.020-1.050 g/ml (Xian P. et al. 2023). Even though, the presence of silicified cell walls makes diatoms more resistant to turbulence in the ocean than other phytoplankton (Verma, J. et al. 2023), the density of the silicified cell walls (also known as frustules) which has density of 1.400-2.200 g/ml (Hamano R. et al. 2021), challenges cells to stay in the water without sinking. As the probability of sinking in water increases, having more chitin nanofibers, which have a density of 1.000-1.300 g/ml (Tarpichai, S. et al. 2023), attached to the cell wall may help the cells protect their position in the water

column to access sufficient sunlight and nutrients.

The findings of previous studies show that various abiotic stress conditions including deficiency of critical nutrients (e.g. silicon and iron) induce expression of genes encoding chitin synthase (Wustmann, M. et. al. 2020, Hildebrand, M. et al. 2018 and Davis, A.K. et al. 2015) The presence of chitin synthase genes does not necessarily indicate the chitin production capability of diatom species. Even though the genome of *Phaeodactylum tricornutum* contains all genes associated with chitin synthesis, there is no evidence of chitin fiber secretion by this species (Durkin C.A. et al. 2009). Therefore, it is critical to measure the actual chitin productivity.

Heretofore, studies conducted to develop data for commercial scale diatom-based chitin production have examined the effects of various factors such as light intensity, nutrient regime shifts and strain selection. For instance, Ozkan and Rorrer examined the effects of multistage silicon and nitrate addition process on chitin nanofiber productivity of the diatom *Cyclotella cryptica* UTEX 1269 and reported that final chitin concentration up to 700 mg/L was obtained after multistage addition of silicon, 19 mmol/L in total and nitrate, 31 mmol/L in total (Ozkan and Rorrer, 2017). In another study by Ozkan and Rorrer, the effects of exposure to different light intensities (35  $\mu$ E/m<sup>2</sup>s, 70  $\mu$ E/m<sup>2</sup>s, 220  $\mu$ E/m<sup>2</sup>s, 370  $\mu$ E/m<sup>2</sup>s and 520  $\mu$ E/m<sup>2</sup>s) on the chitin nanofiber productivity of marine diatom *Cyclotella* were investigated and it has been revealed that the final chitin yield per cell basis was not directly correlated with the changes in light intensity (Ozkan and Rorrer, 2017). Ozkan and Rorrer also showed that cultivation with different levels of dissolved carbon dioxide (200, 800, 2000 and 3000 ppm) availability does not markedly influence the chitin productivity of the diatom *Cyclotella cryptica* UTEX 1269 (Ozkan & Rorrer, 2017).

In 2019, LeDuff and Rorrer analyzed chitin nanofiber productivity of the diatom *Cyclotella cryptica* UTEX 1269 cultivated in a bubble-column reactor operated in batch mode, aerated with 0.1 vvm and exposed to shear rate of 5 s<sup>-1</sup> (according to the calculations based on the equations developed by Nishikawa et al.). The final chitin concentration was 13 mg/L for low silicon concentration (initially added amount was 0.25 mM), when the amount of silicon added to the culture raised to 1.7 mM, the reported final chitin concentration was 77 mg/L (LeDuff and Rorrer, 2019). This study aims to cover the literature gap by addressing the effects of exposure to different shear rates on chitin productivity of the diatom *Cyclotella cryptica*.

# CHAPTER 2

## MATERIALS AND METHODS

### 2.1. Preparation of Culture Media

The diatom *Cyclotella cryptica* CCMP 333 was cultivated in Harrison's and Guillard's f/2 enrichment artificial seawater medium, detailed information regarding ingredients including major nutrients, salts, trace metals and vitamins are provided in the tables which can be found in the appendix A. (Guillard and Ryther 1962).

### 2.2. Photobioreactor Setup & Process Parameters

The diatom *Cyclotella cryptica* CCMP 333 was autotrophically cultivated in a bubble column photobioreactor which consisted of a glass cylinder (with inner diameter of 13.5 cm) placed between circular stainless-steel plates (type 316) and surrounded with tungsten halogen lamp towers from 4 different sides (Figure 2.1.). Considering the results of previous studies proving the efficiency of two-stage cultivation protocol (primarily silicon deplete condition with low light intensity and later silicon dosaging at increased light intensity) was followed for maximization of chitin productivity. Photosynthetically active radiation sensors are used to ensure that targeted light intensity values are reached. Carbon dioxide was supplied through a 4-hole diffuser located at the bottom of the reactor. The diameter of each bubble hole in the diffusers was identical and equal to 1 mm. The carbon dioxide composition in the aeration gas was kept constant at 2% (volume/volume) by using two distinct mass flow controllers for the air compressor and the carbon dioxide tank. The air supplied to the reactor was sterilized with a 0.22  $\mu\text{m}$  pore

sized high efficiency particulate air filter. To maintain sufficient moisture content, the air was passed through 2 consecutive bottles containing sterile distilled water before entering the reactor. Temperature of the growth media was kept constant at 25 °C by utilizing a U-shape pipe connected to a water circulator chiller.

The average shear rate in the bubble column photobioreactor was calculated by using the following equation developed by Nishikawa et al. (Chisti, Y. & Moo-Young, M. 1989)

$$\gamma' \text{ (average shear rate)} = 5000 \times U_G \text{ (theoretical superficial gas velocity)}$$

Table 2.1. Process conditions of the photobioreactor cultivation experiments

Cultivation Temperature	25 ( $\pm 1$ ) °C
Initial Culture Volume	4 L
Aeration Gas Flow Rate for Stage I	0.5 vvm
Aeration Gas Flow Rate for Stage II	0.25 vvm / 1 vvm / 1.5 vvm
Average Shear Rate for Stage II	5.83 s <sup>-1</sup> / 23.31 s <sup>-1</sup> / 34.97 s <sup>-1</sup>
Initial Si Concentration (Stage I)	0.20 mM
Initial Si Concentration (Stage II)	1.80 mM
Average Incident Light Intensity (Stage I)	100 $\mu\text{mol}/\text{m}^2\text{.sec}$
Average Incident Light Intensity (Stage II)	435 $\mu\text{mol}/\text{m}^2\text{.sec}$
Photoperiod (Light : Dark)	14:10

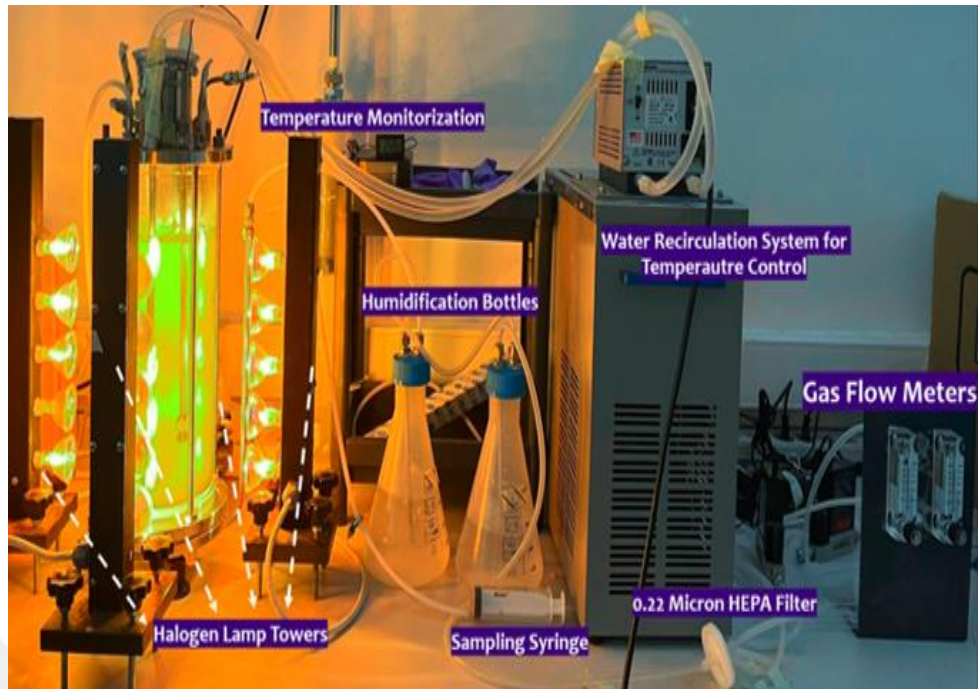


Figure 2.1. Photobioreactor setup used for *Cyclotella cryptica* cultivation.

### 2.3. Dissolved Nutrient Concentration Measurements.

Three different spectrophotometric measurements were conducted in samples taken from the PBR reactor to monitor cell growth and nutrient consumption on a daily basis. The optical density of the suspension was measured at 750 nm. Samples taken from the photobioreactor were centrifuged at 2000 g for 10 minutes to obtain supernatants to be used in spectrophotometric measurements of dissolved nutrients. The dissolved silicon concentration in the sample was measured at 360 nm after the addition of 0.1 mL 18% hydrochloric acid solution and 0.2 mL 115 mM ammonium molybdate solution to 5 ml (Fanning, K. & Pilson, M. 1971). The dissolved nitrate concentration of the sample was measured at 220 nm wavelength (Collos Y. & Slawyk, G, 1976)

## 2.4. Cell Number Density Measurements

Cell growth was followed by using a hemocytometer which had a depth of 200  $\mu\text{m}$  under the light microscope (Nikon Eclipse Ei). The cell number densities were calculated by dividing the number of counted cells to the total scanned area and hemocytometer depth. Live and dead cell distinguishment was ensured by following Evans blue (CAS 314-13-6) staining protocol. (Garrison and Tang 2014). Since the dye cannot infiltrate into the live and healthy cells with intact membranes, dead cells appear in blue.

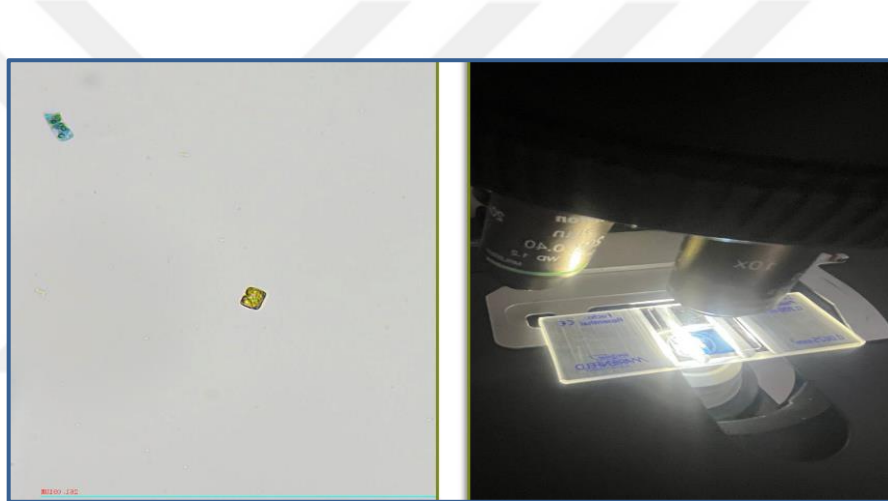


Figure 2.2. The appearance of Evans Blue on Thoma chamber and stained cells.

## 2.5. Chitin Nanofiber Concentration Measurements

The chitin nanofiber concentration of the samples was calculated by dividing the total mass of chitin nanofiber to total volume of the sample and the dilution factor. Since the shape of the nanofibers are cylindrical, the mass of each nanofiber was calculated by multiplying the chitin density, which is equal to 1495  $\text{mg}/\text{cm}^3$  (Dweltz, N.E. et al. 1968), to fiber volume which was calculated by multiplying  $\pi$  number, square of average fiber radius and total cumulative length of the fibers in the sample (Özkan, A. 2023). To prevent

deterioration of image quality by impurities such as salt residues, samples were washed with nanopure water and then centrifugated at 16,000 for 30 minutes to ensure that all chitin nanofibers precipitate to the bottom (LeDuff, P. & Rorrer, G. 2019). After discarding the supernatant, nanopure water was added onto the precipitate for making the final sample volume equal to the initial sample volume.

Following serial dilutions that allow examination of each fiber individually through the Image J software, samples were pipetted onto glass slides for obtaining images through differential interference contrast microscopy for fiber length measurement and pipetted onto aluminum foil, which was subjected to sputter coating with gold after drying of the sample, for obtaining images through scanning electron microscopy (Fei Quanta, 250 FEG) to measure fiber diameters individually.

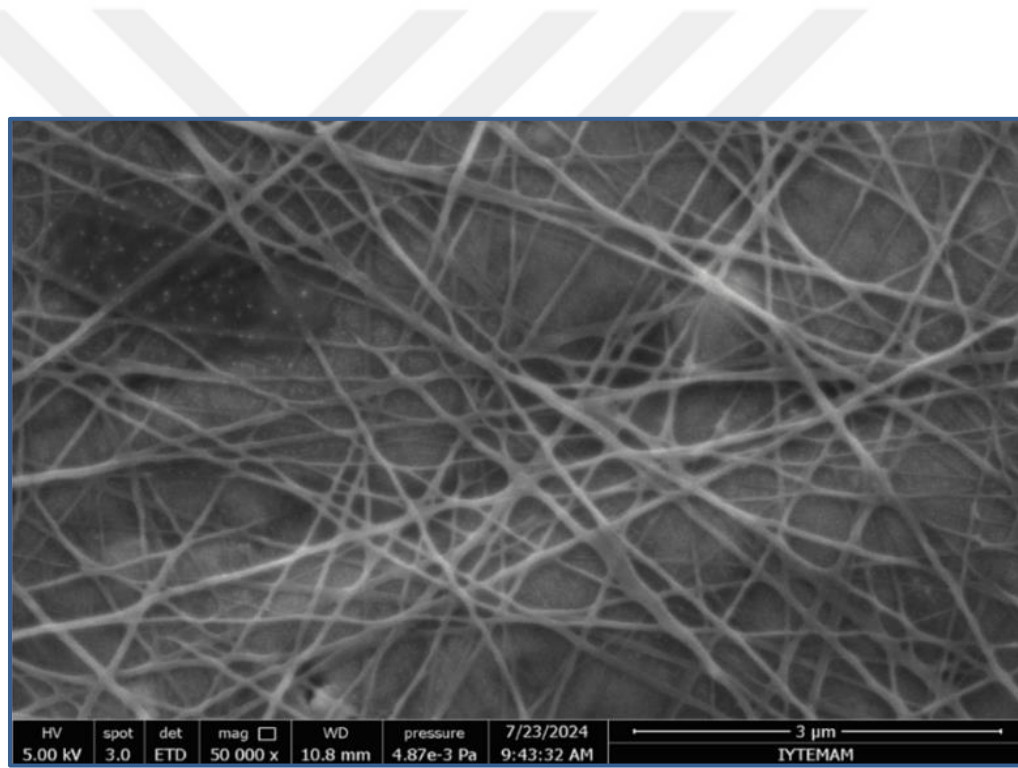


Figure 2.3. Chitin nanofiber images obtained by scanning electron microscopy.

## 2.6.Determination of Cell Bound and Free Chitin Concentrations

The concentrations of free chitin and cell bound chitin in suspension were determined by manually counting and measuring the length of fibers in samples intentionally prepared without centrifugation considering the possibility that centrifugal force may tear off some of the chitin nanofibers originally attached to cells. Exemplary images obtained by differential interference contrast microscopy are presented below to show dislodged chitin nanofibers (Figure 2.4.) and cell-bound chitin nanofibers (Figure 2.5.).



Figure 2.4. Dislodged chitin nanofibers.

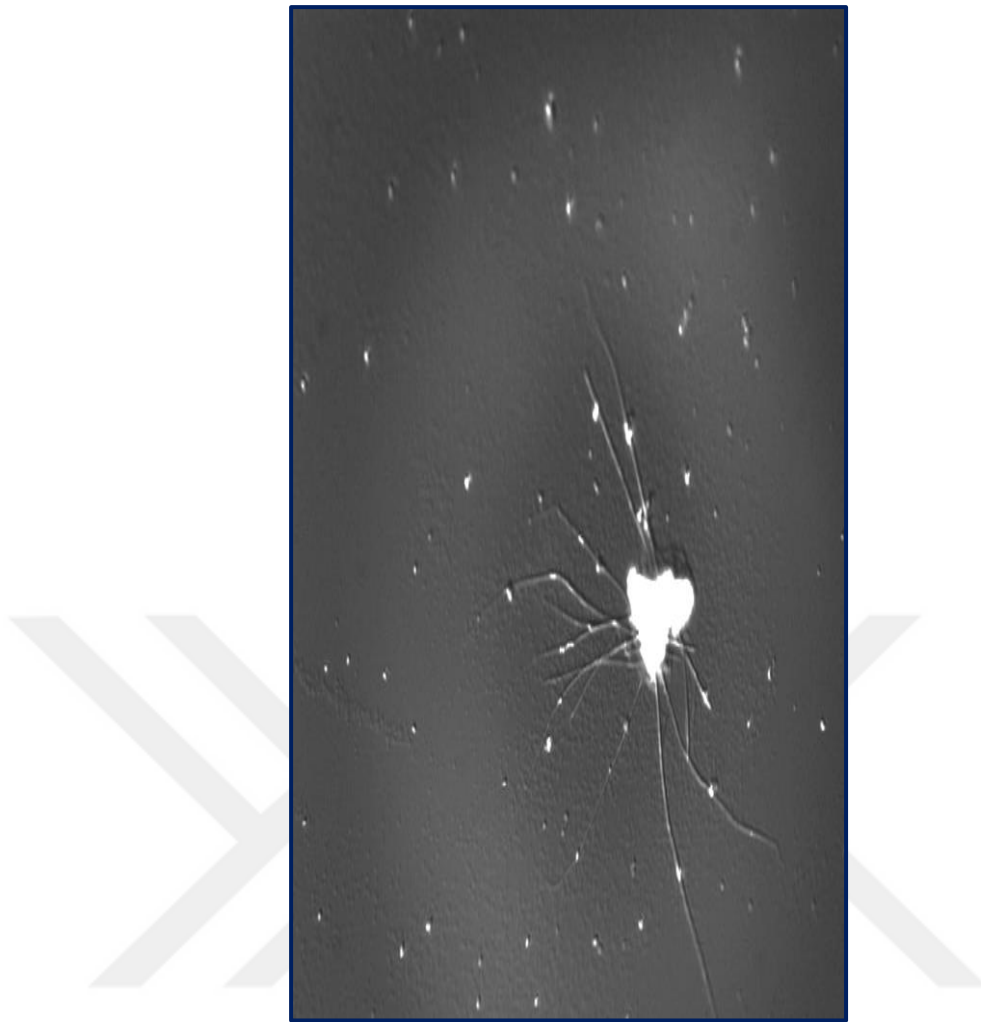


Figure 2.5. Cell bound chitin nanofibers.

## CHAPTER 3

## RESULTS & DISCUSSION

### 3.1. Effects of Different Gas Flow Rates on Cell Density

The changes in cell number density with respect to time are shown in Figure 3.1. The points marked in pink point to the timing of complete consumption of dissolved silicon in the cultivation media. At flow rates of 0.25 vvm and 1 vvm, dissolved silicone was consumed in 2 days while for cell culture aerated with the flow rate of 1.5 vvm, it took 6 days for the silicone to be completely consumed. Considering microhydrodynamic conditions, the highest gas aeration flow rate (1.5 vvm) condition may have caused the exceedance of mechanical stress endurance limits of the *Cyclotella cryptica* cells and reduced nutrient use efficiency. The highest cell number density was reached during the 1 vvm gas aeration flow rate condition.

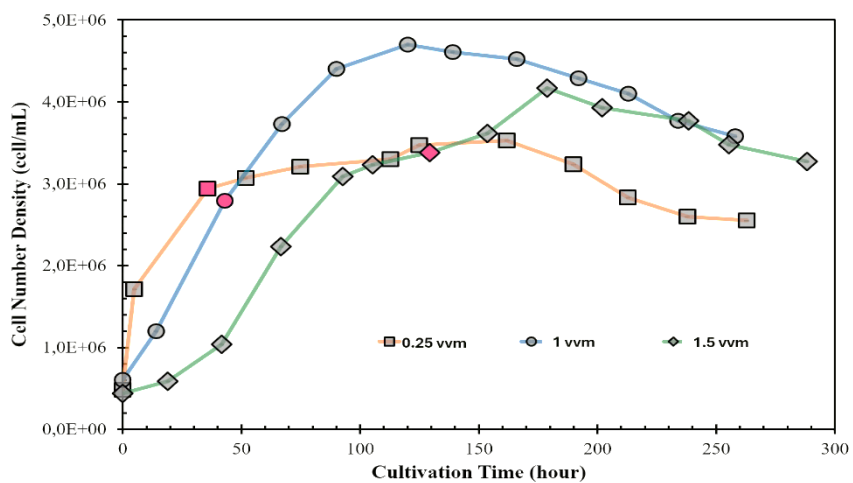


Figure 3.1. Cell number density vs. cultivation time for all gas flowrates.

### 3.2. Effects of Different Gas Flowrates on Chitin Productivity

Chitin productivity was evaluated based on calculations obtained by dividing the amount of total chitin in the suspension to the cell number density. At the end of the two-stage cultivation protocol, 852 mg/L was the highest final chitin concentration obtained from the *Cyclotella cryptica* suspension aerated with 1 vvm flow rate. The second highest final chitin concentration was 502 mg/L and obtained from the *Cyclotella cryptica* suspension aerated with 0.25 vvm flow rate. The lowest final chitin concentration was 213 mg/L and obtained from the *Cyclotella cryptica* suspension aerated with 1.5 vvm and has the the highest amount of foam accumulation.

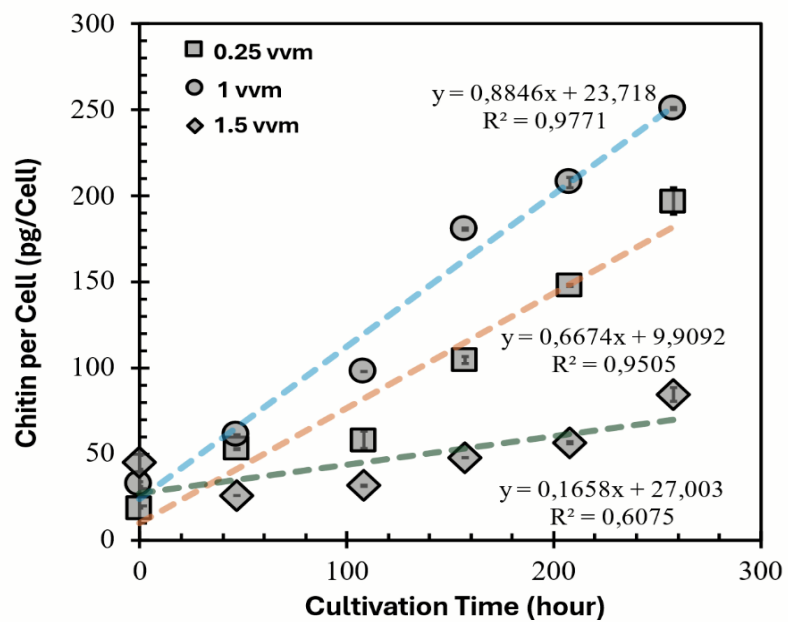


Figure 3.2. Chitin production per cell vs. time for different aeration gas flow rates.

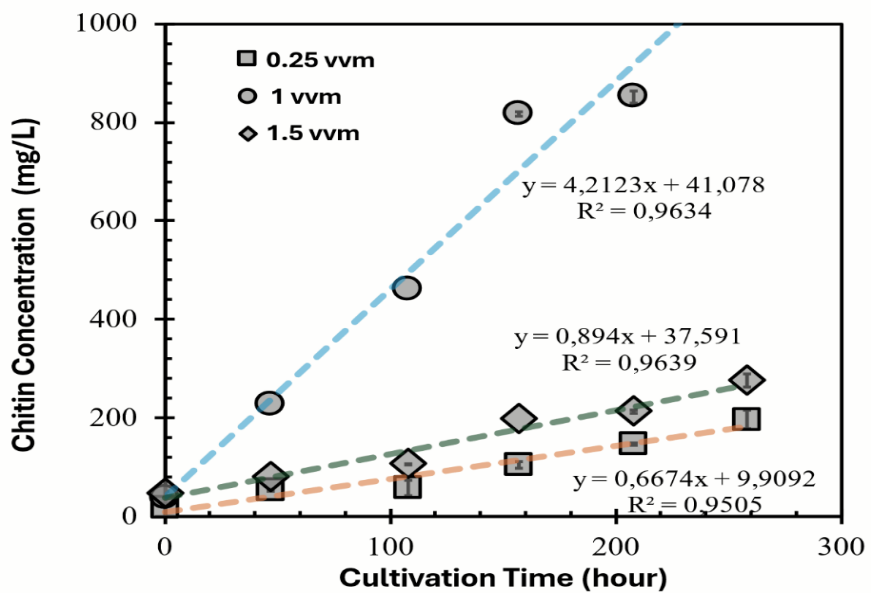


Figure 3.3. Chitin concentration with respect to cultivation time.

### 3.3. Chitin Nanofiber Diameter and Length Distributions

The average diameters of chitin nanofibers extruded by *Cyclotella cryptica* were determined 73.18 nm (n=198) for the cultivation media aerated with the flowrate of 0.25 vvm, 78.69 nm (n=178) for the cultivation media aerated with the flowrate of 1 vvm and 77.10 nm (n=173) for the cultivation media aerated with the flowrate of 1.5 vvm. According to the results of the statistical analyses performed by using Jamovi software version 2.3.28, the variation in gas aeration rate did not have a statistically significant effect on the diameters of the chitin nanofibers secreted by *Cyclotella cryptica* cells (p value > 0.05).

The average length of chitin nanofibers collected from *Cyclotella cryptica* suspensions aerated with different rates (0.25 vvm, 1 vmm and 1.5 vvm) during different periods of cultivation are given in table 3.1. The variations in the length of chitin nanofibers collected from the *Cyclotella cryptica* suspension aerated with 0.25 vvm, 1 vvm and 1,5 vvm are separately shown in Figure 3.5, Figure 3.6. and Figure 3.7. on the following pages.

Table 3.1. Average chitin nanofiber length during photobioreactor cultivation at different aeration gas flow rates

Aeration Rate (vvm)	0.25	1	1.5
Time Elapsed			
After Addition of Silicone (hr)			
24	14.26 nm	15.87 nm	12.91 nm
72	16.68 nm	15.92 nm	14.46 nm
120	17.25 nm	14.74 nm	13.46 nm
168	15.74 nm	15.41 nm	13.17 nm
216	16.21 nm	14.13 nm	11.17 nm
264	16.17 nm	15.50 nm	11.45 nm

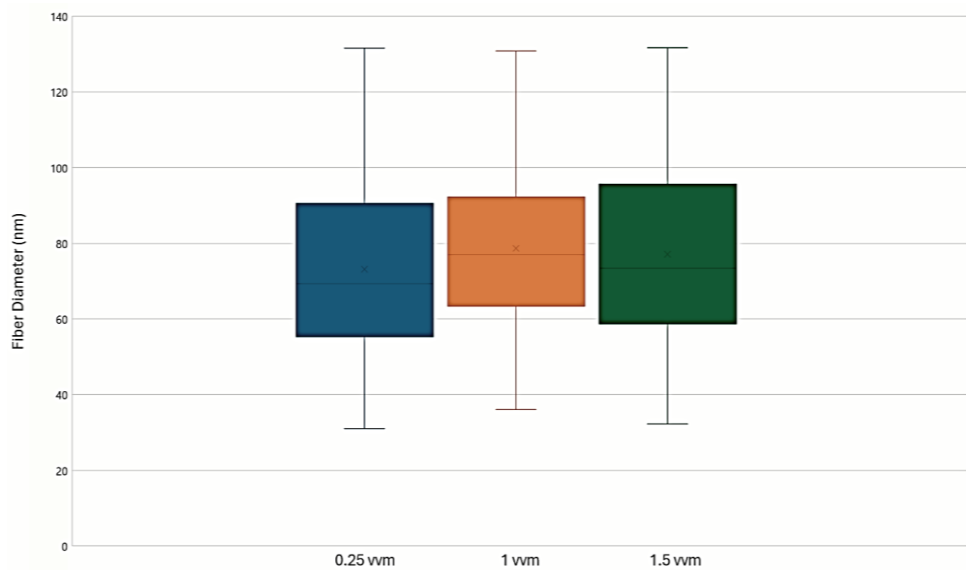


Figure 3.4. Boxplot distribution of the diameters of chitin nanofibers secreted by *Cyclotella cryptica* cells during cultivation at different aeration gas flowrates.

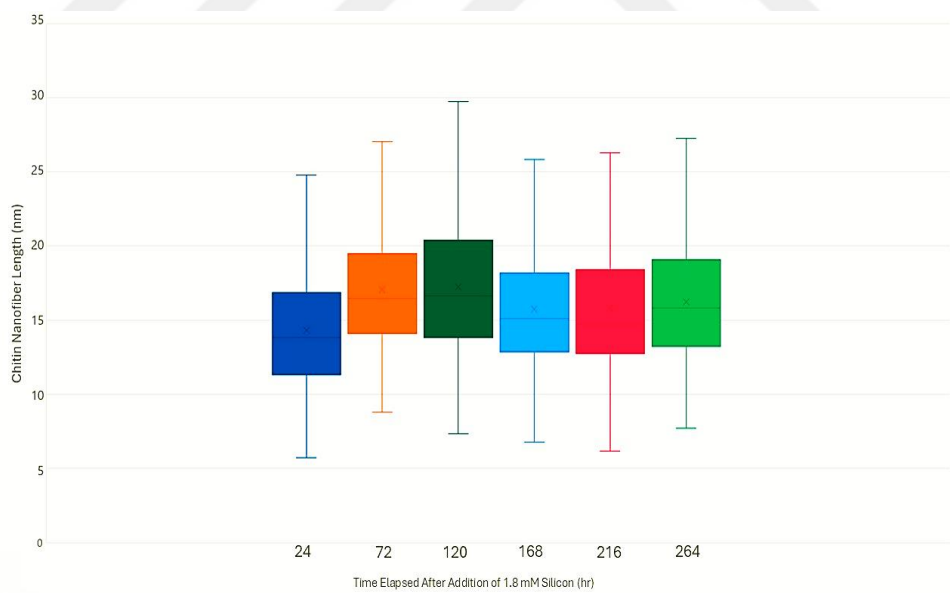


Figure 3.5. Boxplot distribution of the lengths of chitin nanofibers secreted by *Cyclotella cryptica* cells during cultivation at 0.25 vvm.

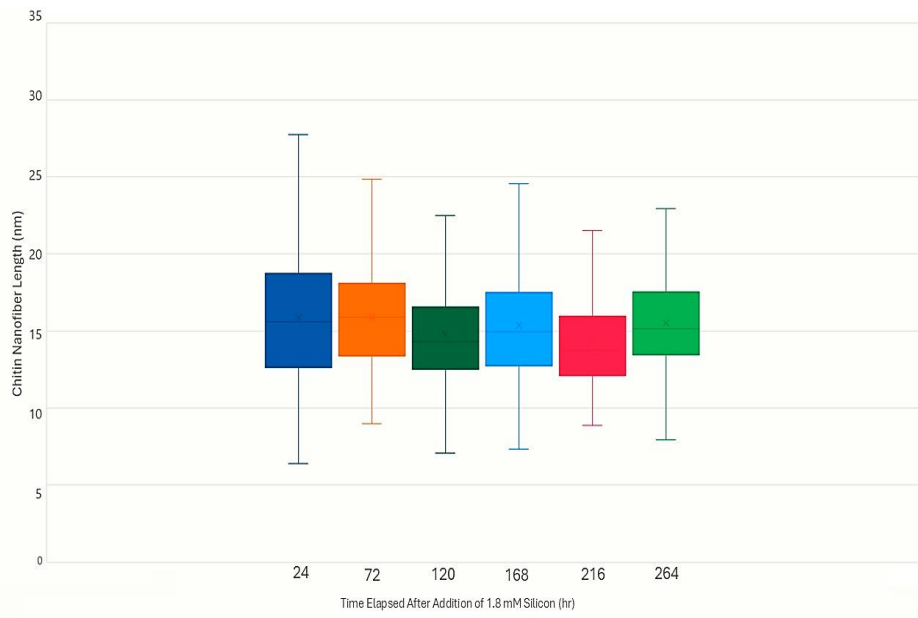


Figure 3.6. Boxplot distribution of the lengths of chitin nanofibers secreted by *Cyclotella cryptica* cells during cultivation at 1 vvm.

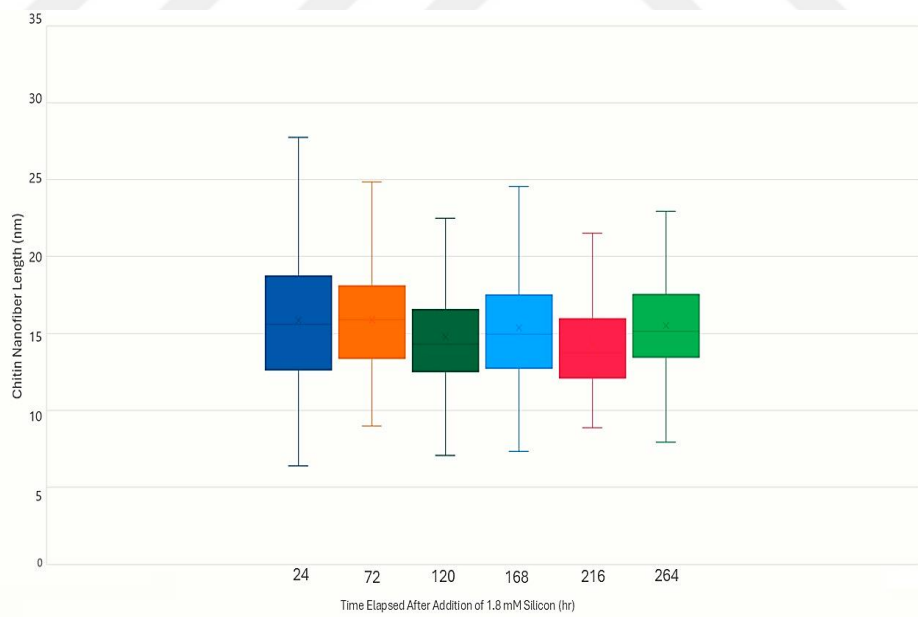


Figure 3.7. Boxplot distribution of the lengths of chitin nanofibers secreted by *Cyclotella cryptica* cells during cultivation at 1.5 vvm.

The lengths of chitin nanofibers were shorter after exposure to 1.5 vvm, when compared to exposure to 0.25 vvm and 1 vvm in all time periods. This may be explained by the hypothesis that higher shear exposure reduces the retention of fibers and causes them to dislodge before they can grow longer. However, according to the results of the statistical analyses performed by using Jamovi software version 2.3.28, the variation in gas aeration rate does not have a statistically significant effect on the lengths of the chitin nanofibers secreted by *Cyclotella cryptica* cells during different amounts of time elapsed after addition of 1.8 mM silicon (p value > 0.05).

### **3.4. Effects of Different Gas Flow Rates on Fultoportulae Number**

The average numbers of fultoportulae found on the *Cyclotella cryptica* cells were calculated by analyzing images obtained through scanning electron microscopy. The average number of fultoportulae is equal to 22.33 (n=12) for the cells exposed to 0.25 vvm, 23.40 (n=10) for the cells exposed to 1 vvm and 23.25 (n=7) for the cells exposed to 1.5 vvm.

### **3.5. Effects of Different Gas Flow Rates on the Concentrations of Cell Bound Chitin Nanofibers and Free Chitin Nanofibers**

The maximum cell-bound chitin nanofiber to total chitin nanofiber ratio was equal to 15.5% and detected in the sample collected from the reactor aerated with 0.25 vvm. Under the same conditions, cell bound chitin nanofiber to total chitin nanofiber ratio decreased from 15.5% to 9%, as aeration gas flowrate increased from 0.25 vvm to 1 vvm. The samples collected during the same interval of stationary phase (stage 2, day<sup>7</sup>) from all three cell suspensions started with the same initial cell densities and same process conditions, reveal inverse proportion between cell bound chitin nanofiber to total chitin nanofiber ratio and gas flowrate.

As shown in Figure 3.8., the cell-bound chitin nanofiber ratios of the samples

collected from the reactor on the 7<sup>th</sup> day of the second cultivation stage (stationary phase) reveal the direct proportion (95.7% free fibers for 1.5 vvm, 93.6% for 1 vvm and 91% for 0.25 vvm) between free circulation of chitin nanofibers and increased aeration flow rate.

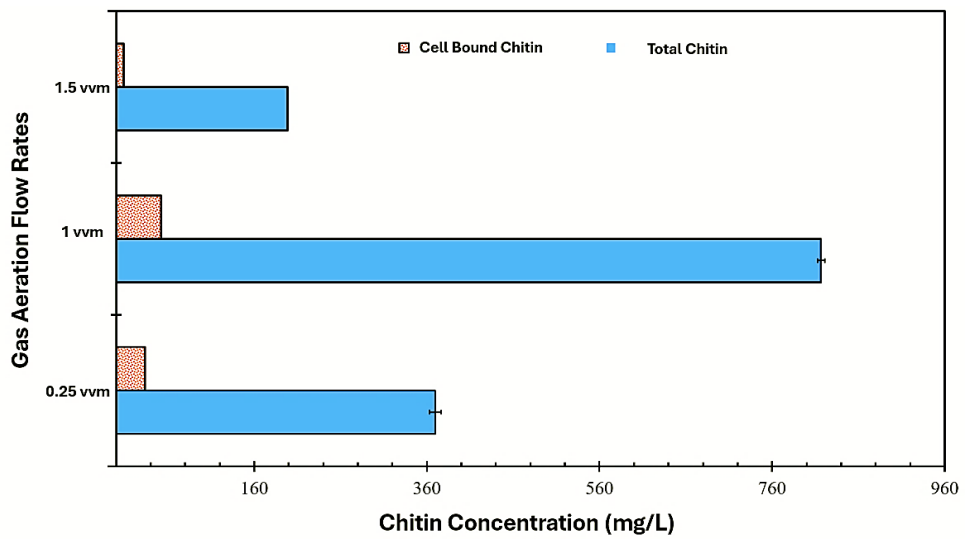


Figure 3.8. Concentrations of cell bound and free chitin nanofibers at different aeration gas flow rates.

## CHAPTER 4

### CONCLUSION

Yield enhancement strategies for commercialization of diatom-based chitin nanofiber production systems are important to compensate for rising demand for high quality chitin nanofibers by the biomedical industry. In this study, the effects of variation in aeration-induced shear rate have on the chitin nanofiber productivity of diatom *Cyclotella cryptica* CCMP 333 were investigated by following a two-stage cultivation procedure that requires application of silicon deplete and replete conditions consecutively. The addition of silicone during transition from stage I to stage II increased the chitin productivity in all experimental groups exposed to different aeration rates. The amount of silicon and all other nutrients added, and the time of nutrient addition were kept same in all experimental groups.

The lowest chitin nanofiber productivity was obtained after increasing the aeration rate from 0.5 vvm to 1.5 vvm while transitioning from stage I to stage II. Decreasing the aeration rate from 0.5 vvm to 0.25 vvm while transitioning from stage I to stage II provided better productivity than the experimental group exposed to shift from 0.5 vvm to 1.5 vvm, and lower productivity than the experimental group exposed to shift from 0.5 vvm to 1 vvm. Chitin nanofiber productivity of *Cyclotella cryptica* CCMP 333 cells was maximized by increasing the aeration rate from 0.5 vvm to 1 vvm while transitioning from the stage I to stage II.

The variation in gas aeration rate did not have a statistically significant effect on the lengths and diameters of the chitin nanofibers secreted by *Cyclotella cryptica* CCMP 333 cells. Similarly, the variation in gas aeration rate did not change the average number of fultoportulae found on the frustules of *Cyclotella cryptica* CCMP 333 cells. Therefore, it has been shown that the increase in chitin productivity is not related to structurally having more fultoportulae on the frustule. Exposing different shear rates changes the amount of chitin nanofiber secreted from each fultoportula. However, the molecular mechanisms behind this finding have not been fully disclosed yet. As pointed out by the

previous publications in the literature, it is not always possible to find a positive correlation between the presence and increased expression of genes associated with chitin synthesis and the actual chitin productivity of diatom species. From this point on development of harvesting strategies based on actual chitin productivity characteristics of diatom species gains importance. This study revealed that as the exposed shear rate increases, the detachment ratio of chitin nanofibers from cells also increases.

Although the highest free fiber ratio was found in the samples collected from the experimental setup with the highest gas aeration rate (1.5 vvm), exceeding a certain threshold of shear rate exposure reduces the total chitin productivity of the *Cyclotella cryptica* CCMP 333 cells. These findings should be taken into consideration when scaling up diatom cultivations to the large volumes required for commercial production of high-quality chitin nanofibers.

## REFERENCES

Abidin, Nurul Ayani Zainol, Kormin, Faridah, Abidin Nurul Akhma Zainol, Anuar, Nor Aini Fatihah Mohamed and Bakar, Mohd Fadzelly Abu Bakar. 2020. “ The potential of insects as alternative sources of chitin: an overview on the chemical method of extraction from various sources.” *Int. J. Mol. Sci.* 21(14):4978. <https://doi.org/10.3390/ijms21144978>.

Aranaz, Imaculada, Mengibar, Marian, Harris, Ruth, Panos, Ines. 2019. “Functional Characterization of Chitin and Chitosan.” *Current Chemical Biology*. 3(2):203-230. <https://doi.org/10.2174/187231309788166415>

Beniash, Elia, Ivanina Anna, Lieb, Nicholas, Kurochkin Ilya, Sokolava, Inna. 2010. “Elevated level of carbon dioxide affects metabolism and shell formation in oysters *Crassostrea virginica*” *MEPS*. 419: 95-108. <https://doi.org/10.3354/meps08841>

Berroci, Maria, Vallejo Claudia, Lizundia Erlantz. 2022. “Environmental Impact Assessment of Chitin Nanofibril and Nanocrystal Isolation from Fungi, Shrimp Shells and Crab Shells” *ACS Sustainable Chemistry & Engineering*. <https://doi.org/10.1021/acssuschemeng.2c04417>

Chisti, Yusuf and Moo-Young, Murray. 1989. “On the calculation of shear rate and apparent viscosity in airlift and bubble column bioreactors.” *Biotechnology and Bioengineering*. 34(11): 1391-1392. <https://doi.org/10.1002/bit.260380214>.

Chitin Prices, ChitoLytic. Retrieved from: [chitolytic.com/chitosan\\_products/chitin-supply/](http://chitolytic.com/chitosan_products/chitin-supply/) Access Date: October 5<sup>th</sup>, 2024.

Davis, Aubrey., Hildebrand Mark and Palenik Brian. 2005. “Stress Induced Protein Associated with the Girdle Band Region of the Diatom, *Thalassiosira pseudonana*” *J. Phycol.* 41(3): 577-589. <https://doi.org/10.1111/j.1529-8817.2005.00076.x>

Durkin, Colleen, Mock Thomas., Armbrust Viginia. 2009. “Chitin in Diatoms and Its Association with the Cell Wall” *Eukaryotic Cell*. 8(7): 1038-1050. <https://doi.org/10.1128/EC.00079-09>

Dweltz, N.E., Colvin, J.R., McInnes, A.G. 1968. "Studies on chitan ( $\beta$ -(1 → 4)-linked 2-acetamido-2-deoxy-D-glucan) fibers of the diatom *Thalassiosira fluviatilis*, Hustedt. III. The structure of chitan from x-ray diffraction and electron microscope observations." *Canadian Journal of Chemistry*. 68(05):1513-1521. <https://doi.org/10.1139/v68-248>

Feng, Wenjun. & Wang, Zhengke. 2023. "Tailoring the Swelling-Shrinkable Behavior of Hydrogels for Biomedical Applications." *Advanced Science*. 10(28):230326. <https://doi.org/10.1002/advs.202303326>.

Garrison, Haley. & Tang, Kam. 2014. "Effects of episodic turbulence on diatom mortality and physiology, with a protocol for the use of Evans Blue stain for live-dead determinations." *Hydrobiologia*. 738:155-170. <https://doi.org/10.1007/s10750-014-1927-0>

Gooday, Graham, Woodman, Julia, Casson, Elizabeth, Browne, Catherine. 1985. "Effect of nikkomycin on chitin spine formation in the diatom *Thalassiosira fluviatilis*, and observations on its peptide uptake." *FEMS Microbiology Letters*. 28(3):335-340. <https://doi.org/10.1111/j.1574-6968.1985.tb00816.x>

Green, Timothy, Nachson, Siboni, King, William, Labbate, Maurizio, Seymour, Justin, Raftos, David. 2019. "Simulated marine heat wave alters abundance and structure of vibrio populations associated with the pacific oyster resulting in a mass mortality event." *Microbial Ecology*. 77:736-747. <https://doi.org/10.1007/s00248-018-1242-9>.

Gryzunov, S. 2024. Chitin (from Crustacean chitin). VWR International, Retrieved from: [us.vwr.com/store/product/145117/20/chitin-from-crustacean-chitin-brown-powder-unbleached](https://us.vwr.com/store/product/145117/20/chitin-from-crustacean-chitin-brown-powder-unbleached). Access Date: October 5<sup>th</sup>, 2024.

Guillard Robert & Ryther John H. 1962. "Studies of marine planktonic diatoms. I. *Cyclotella nana* and *Detonula confervacea*", *Canadian Journal of Microbiology* 8: 229-239. <https://doi.org/10.1139/m62-029>.

Hamano, Ryo, Shomura, Shingo, Takeda, Yuto, Yamazaki, Tokio, Hirayama Kota., Hanada, Yasutaka, Mayama, Shigeki., Takemura, Masaharu., Lin, Han-Jia., Umemura Kazuo. 2021. "Sinking of Four Species of Living Diatom Cells Directly Observed a Tumbled Optical Microscope", *Microscopy and Microanalysis*. 5(27): 1154-1160. <https://doi.org/10.1017/S1431927621012150>

Hamed, Imen, Özogul Fatih., Regenstein, Joe. 2016. "Industrial applications of crustacean by-products (chitin, chitosan and chito-oligosaccharides)." *Trends in Food Science and Technology*. 48: 40-50.

<https://doi.org/10.1016/j.tifs.2015.11.007>

Hildebrand, Mark., Lerch, Sarah., Shrestha, Roshan. 2019. “Understanding Diatom Cell Wall Silification Moving Forward.” *Front. Mar. Sci.* 5(125). <https://doi.org/10.3389/fmars.2018.00125>

Hou, Jiaxin, Aydemir, Berk Emre, Gümrah-Dumanli, Ahu. 2021. “Understanding the structural diversity of chitins as a versatile biomaterial.” *Phil. Trans. R. Soc. A* 379:20200331, <https://doi.org/10.1098/rsta.2020.0331>

Jeffreys, Clayton, Agathos, Spiros, Rorrer, Gregory. 2015. “Biogenic nanomaterials from photosynthetic microorganisms.” *Current Opinions in Biotechnology.* 33:23-31. <https://doi.org/10.1016/j.copbio.2014.10.00>

Jin, Soo-Ah & Spontak, Richard. 2023. “Fundamentals and Advances in Nanocellulose and Nanochitin Systems”, *Advanced Industrial and Engineering Polymer Research.* 6(4):356-381. <https://doi.org/10.1016/j.aiepr.2023.04.003>

LeDuff, Paul & Rorrer, Greg. 2019. “Formation of extracellular B-chitin nanofibers during batch cultivation of marine diatom *Cyclotella* sp. at silicon limitation.” *Journal of Applied Phycology.* 31:3479-3490. . <https://doi.org/10.1007/s10811-019-01879-6>

Liao, Jing, Zhou, Yuhang, Hou, Bo., Zhang, Jiamin., Huang, Huihua. 2023. “Nano-chitin: Preparation strategies and food biopolymer film reinforcement and applications.” *Carbohydrate Polymers.* 305:120553, . <https://doi.org/10.1016/j.carbpol.2023.120553>

Liu, Yifan, Chen, Long, Meng, Fang., Zhang, Tao., Luo, Jun., Chen, Shuang., Shi, Huilai., Liu, Bingjian., Lv, Zhenming. 2023. “The effect of temperature on the embryo development of cephalopod *Sepiella japonica* suggests crosstalk between autophagy and apoptosis” *Int. J. Mol. Sci.* 24(20):15365. <https://doi.org/10.3390/ijms242015365>

Lubarda, Vlado A. & Asaro, Robert J. 2014. “Viscoelastic Response of Anisotropic Biological Membranes. Part II: Constitutive Models.” *Theoret. Appl. Mech.* 41(3): 213-231. <https://doi.org/10.2298/TAM1403213L>

Mahmood, Hamayoun, Shakeel, Ahmad, Rafique, Sikander, Moniruzzaman, Muhammad. 2022. “Recent progress in ionic liquid assisted processing and extraction of biopolymers”. *Biocatalysis in Green Solvents.* 9:233-255.

<https://doi.org/10.1016/B978-0-323-91306-5.00015-7>

Mario,F.D., Rapana, P., Tomati, U. and Galli, E. 2008. “Chitin and chitosan from Basidiomycetes”. *International Journal of Biological Macromolecules*. 43(1): 8-12. <https://doi.org/10.1016/j.ijbiomac.2007.10.005>.

Miyake, Hiroshi, Tsukhara, Junzo, Hashimoto, Jun, Uematsu, Katsuyuki. and Maruyama, Tadashi. 2006. “Rearing and observation methods of vestimentiferan tubeworm and its early development at atmospheric pressure.” *Cah. Biol. Mar.* 47:471-475. <https://doi.org/10.1186/VLIZ289414>

Moon, Hyunwoo, Choy, Seunghwan, Park, Yeonju, Jung, Young Mee., Koo, Jun Mo., Hwang, Dong Soo. 2019. “Different Molecular Interaction between Collagen and  $\beta$ -Chitin in Mechanically Improved Electrospun Composite”. *Marine Drugs*. 17(6):318. <https://doi.org/10.3390/md17060318>.

Morganti, Pierfrancesco, Muzzarelli, Ricardo A., Muzzarelli, C. 2016. “Multifunctional Use of Innovative Chitin Nanofibrils for Skin Care.” *J. Appl. Cosmetol.* 24, 105-114. [journalofappliedcosmetology.com/post/multifunctional-use-of-innovative-chitin-nanofibrils-for-skin-care](http://journalofappliedcosmetology.com/post/multifunctional-use-of-innovative-chitin-nanofibrils-for-skin-care).

Mouritsen, Ole, Styrbaek, Klavs. 2018. “Cephalopod Gastronomy – A Promise for the Future.” *Frontiers in Communication*, 3(38). <https://doi.org/10.3389/fcomm.2018.00038>

Yadav, Monila, Priyhnshi, Goswami, Paritosh, Kunwar, Kumar, Manish, Pareek Nidhi, Vivekanand Vivekanand. 2019. “Seafood Waste: A Source for Preparation of Commercially Employable Chitin/Chitosan Materials” *Bioresources and Bioprocessing*, 6:8. <https://doi.org/10.1186/s40643-019-0243-y>

Ozkan, Altan. 2023. “Screening diatom strains belonging to *Cyclotella* genus for chitin nanofiber production under photobioreactor conditions: Chitin productivity and characterization of physicochemical properties”, *Algal Research*, 70:103015. <https://doi.org/10.1016/j.algal.2023.103015>

Ozkan, Altan & Rorrer, Greg. 2017. “Effect of light intensity on the selectivity of lipid and chitin nanofiber production during photobioreactor cultivation of the marine diatom *Cyclotella* sp.” *Algal Research*, 25: 216-227. <https://doi.org/10.1016/j.algal.2017.04.032>

Ozkan, Altan & Rorrer, Greg. 2017. “Effects of CO<sub>2</sub> delivery on fatty acid and chitin

nanofiber production during photobioreactor cultivation of the marine diatom *Cyclotella* sp.” *Algal Research* 25:422-430. <https://doi.org/10.1016/j.algal.2017.07.003>

Ozkan, Altan & Rorrer, Greg. 2017. “Lipid And Chitin Nanofiber Production During Cultivation of The Marine Diatom *Cyclotella* Sp. to High Cell Density With Multistage Addition of Silicon and Nitrate.” *Journal of Applied Phycology*, 29:1811-1818. <https://doi.org/10.1007/s10811-017-1113-7>

Raabe, D., Sawalmih, A., Yi, S.B., Fabritius, H. 2007. “Preferred crystallographic texture of  $\alpha$ -chitin as a microscopic and macroscopic design principle of the exoskeleton of the lobster *Homarus americanus*.” *Acta Biomaterials*. 3: 882-895. <https://doi.org/10.1016/j.actbio.2007.04.006>

Rajan, Durairaj Karthick, Mohan, Kannan, Rajarajeswaran, Jayakumar, Divya, Dharmaraj, Kumar, R.agavendhar, Kandasamy, Sabariswaran, Zhang, Shubing, Ganesan, Abirami Ramu Ganesan. 2023. “ $\beta$ -Chitin and chitosan from waste shells of edible mollusks as a functional ingredient”. *Food Frontiers*. 5(1):46-72. <https://doi.org/10.1002/fft2.326>

Romay, Aarion, Payne, Gregory, Shen, Jana. 2023. “Mechanism of the Temperature-Dependent Self Assembly and Polymorphism of Chitin” *Chemistry of Materials*. 35(16):6472-6481. <https://doi.org/10.1021/acs.chemmater.3c01313>

Rosa, Rui, Pimentel, Marta., Boavida-Portugal, Joana, Teixeira, Tatiana, Trübenbach, Katja, Diniz, Mario. 2012. “Ocean warming enhances malformations, premature hatching, metabolic suppression and oxidative stress in the early life stages of a keystone squid.” *PLoS ONE* 7(6): e38282 <https://doi.org/10.1371/journal.pone.0038282>

Rousseaux, Cecile & Gregg Watson. 2014. “Interannual Variation in Phytoplankton Primary Production at A Global Scale.” *Remote Sens.* 6(1):11-19. <https://doi.org/10.3390/rs6010001>

Sharma, Nikunj, Simon, Daris Pazhukkunnel, Diaz-Garza, Aracely, Maribel, Fantino Elisa, Messaabi Anis, Meddeb-Mouelhi, Fatma, Germain, Hugo, Desgagne-Penix, Isabel. 2021. “Diatoms Biotechnology: Various Industrial Applications for a Greener Tomorrow.” *Frontiers in Marine Science*. 8: 636613. <https://doi.org/10.3389/fmars.2021.636613>

Smith, Carr, Vournakis, John, Demcheva, Marina, Fischer Thomas. 2008. “Differential Effect of Materials for Surface Hemostasis on Red Cell Blood Morphology.”

Sulthan, Rashid, Sambhudevan, Sreedha, Greeshma, S., Gayathri, S., Anagha, D.A., Niranjan, B., Gayathri, K., Unni, Vaani. 2023. “Extraction of  $\beta$ -chitin using deep eutectic solvents for biomedical applications.” *Materials Today*. 94:44-48. <https://doi.org/10.1016/j.matpr.2023.05.521>

Tanpitchai, Supachok, Pumpuang, Laphaslada., Srimarut, Yanee, Woraprayote, Weerapong, Malila, Yuwares. 2023. “Development of Chitin Nanofiber Coatings for Prolonging Shelf Life and Inhibiting Bacterial Growth on Fresh Cucumbers”. *Scientific Reports*. 13: 13195. <https://doi.org/10.1038/s41598-023-39739-6>.

Vidal, Erica, Villanueva, Roger, Andrade, Jose., Gleadall, Ian., Iglesias, Jose, Koueta, Noussithe, Rosas, Carlos, Segawa, Susumu, Grasse, Bret, Franco-Santo Rita M., Albertin, Caroline B., Caamal-Monsreal, Claudia, Chimal, Maria, E., Edsinger-Gonzales, Eric, Gallardo, Pedro., Pabic, Charles, Pascual, Cristina, Roumbeda, Katina, Woodret, James. 2014. “Cephalopod Culture: Current Status of Main Biological Models and Research Priorities.” *Advances in Marine Biology*. 67: 1-98. <https://doi.org/10.1016/B978-0-12-800287-2.00001-9>.

Wang, Jaw-Kai & Seibert, Michael. 2017. “Prospects for Commercial Production of Diatoms.” *Biotechnology for Biofuels* 10 (16). <https://doi.org/10.1186/s13068-017-0699-y>

Wustmann, Martin, Poulsen Nicole, Kröger, Nils and Pee, Karlheinz. 2020. “Chitin synthase localization in the diatom *Thalassiosira pseudonana*” *BMC Materials*., 2(10). <https://doi.org/10.1186/s42833-020-00016-9>

Wysokowski, Marcin, Petrenko, Iaroslav, Stelling, Allison, Stawski, Dawid, Jasionowski, Teofil, Ehrlich, Hermann. 2015. “Poriferan Chitin as a Versatile Template for Extreme Biomimetics.” *Polymers*. 7(2):235-265. <https://doi.org/10.3390/polym7020235> .

Xian, Pengfei, Ji, Bing, Bian, Shaofeng, Zong, Jingwen, Zhang, Tao. 2023. “Influence of Differences in the Density of Seawater on the Measurement of the Underwater Gravity Gradient”, *Sensors*. 23(2): 714. <https://doi.org/10.3390/s23020714>

Xie, Ge, Zhou, Nuoya, Du, Shuo, Gao, Yujie, Suo, Huinan, Yang, Jing, Tao, Juan, Zhu, Jintao, Zhang, Lianbin. 2022. “Transparent photothermal hydrogels for wound visualization and accelerated healing.” *Fundamental Research*. 2(2):268-275. <https://doi.org/10.1016/j.fmre.2021.10.001>

Yu, Ailing, Beck, Marius, Merzendorfer, Hans, Yang, Qing. 2024. "Advances in understanding insect chitin biosynthesis." *Insect Biochemistry and Molecular Biology*. 164:104058. <https://doi.org/10.1016/j.ibmb.2023.104058>

Zhao, Xiaming, Zhang, Jianzhen, Zhu, Kun Yan. 2019. "Chito-Protein Matrices in Arthropod Exoskeletons and Peritrophic Matrices." *Extracellular Sugar-Based Biopolymer Matrices*. 1: 3-56. [https://doi.org/10.1007/978-3-030-12919-4\\_1](https://doi.org/10.1007/978-3-030-12919-4_1)



## APPENDIX A

Table A.1. Salts Added to the Culture Media

Formula	Name
NaCl	Sodium chloride
Na <sub>2</sub> SO <sub>4</sub>	Sodium sulfate
KCl	Potassium chloride
NaHCO <sub>3</sub>	Sodium bicarbonate
KBr	Potassium bromide
H <sub>3</sub> BO <sub>3</sub>	Boric acid
NaF	Sodium fluoride
MgCl <sub>2</sub>	Magnesium chloride
CaCl <sub>2</sub>	Calcium chloride
SrCl <sub>2</sub>	Strontium chloride

Table A.2. Trace Metals Added to the Culture Media

Formula	Name
FeCl <sub>3</sub> 6H <sub>2</sub> O	Iron (III) chloride hexahydrate
Na <sub>2</sub> EDTA.2H <sub>2</sub> O	Ethylenediaminetetraacetic acid
MnSO <sub>4</sub> .4H <sub>2</sub> O	Manganese (II) sulfate tetrahydrate
ZnSO <sub>4</sub> 7H <sub>2</sub> O	Zinc sulfate heptahydrate
Na <sub>2</sub> MoO <sub>4</sub> 2H <sub>2</sub> O	Sodium molybdate dihydrate
CuSO <sub>4</sub> 5H <sub>2</sub> O	Cooper (II) sulfate pentahydrate
Na <sub>2</sub> SeO <sub>3</sub>	Sodium selenite
CoSO <sub>4</sub> 7H <sub>2</sub> O	Cobalt (II) sulfate heptahydrate
NiCl <sub>2</sub> 6H <sub>2</sub> O	Nickel (II) chloride hexahydrate

Table A.3. Vitamins Added to the Culture Media

Formula	Name	Quantity per L (g)
C <sub>12</sub> H <sub>17</sub> N <sub>4</sub> OS	Thiamine HCl (Vitamin B1)	0.1
C <sub>10</sub> H <sub>16</sub> N <sub>2</sub> O <sub>3</sub> S	Biotin (Vitamin B9)	0.0005
C <sub>63</sub> H <sub>88</sub> CoN <sub>14</sub> O <sub>14</sub> P	Cyanocobalamin (Vitamin B12)	0.0005

Table A.4. Major Nutrients Added to the Culture Media

Formula	Name	Concentration in Initial Inoculum Medium (mM)	Concentration in Main Medium (mM)
NaNO <sub>3</sub>	Sodium Nitrate	5.32	5.32
NaH <sub>2</sub> PO <sub>4</sub> .H <sub>2</sub> O	Sodium Phosphate	0.24	0.24
NaSiO <sub>3</sub> 9H <sub>2</sub> O	Sodium Silicate	0.50	0.20 (nutrient deplete stage) 1.80 (nutrient replete stage)